DNA Gyrase Requires DNA for Effective Two-Site Coordination of Divalent Metal Ions: Further Insight into the Mechanism of Enzyme Action[†]

Claudia Sissi,[‡] Angelita Chemello,[‡] Elena Vazquez,[‡] Lesley A. Mitchenall,[§] Anthony Maxwell,[§] and Manlio Palumbo*[,‡]

Department of Pharmaceutical Sciences, University of Padova, Via Marzolo, 5, 35131 Padova, Italy, and Department of Biological Chemistry, John Innes Centre, Colney, Norwich, NR4 7UH, U.K.

Received March 20, 2008; Revised Manuscript Received June 7, 2008

ABSTRACT: The catalytic properties of DNA gyrase, an A_2B_2 complex, are modulated by the presence of divalent metal ions. Using circular dichroism, protein melting experiments and enzyme activity assays, we investigated the correlation between the A_2B_2 conformation, the nature of the metal ion cofactor and the enzyme activity in the presence and absence of DNA substrate. At room temperature, DNA gyrase structure is not appreciably affected by Ca^{2+} or Mg^{2+} but is modified by Mn^{2+}. In addition, metal ions strongly affect the enzyme's thermal transitions, rendering the A_2B_2 structure more flexible. Using the B subunit, we were able to identify two distinct complexes with manganese ions. The first one exhibits a 1:1 stoichiometry and is not affected by the presence of DNA. The second complex is associated with a large protein structural modification that can be remarkably modulated by addition of the DNA substrate. This behavior is conserved in the reconstituted protein. Studies with two GyrB mutants indicate that Mn^{2+} interference with the TOPRIM region modulates gyrase supercoiling activity. In particular, considering the need for two divalent metal ions for an efficient catalytic cleavage of the phosphodiester bond, our data suggest that residue D500 participates in the first complexation event (DNA-independent), whereas residue D498 is involved mainly in the second process. In conclusion, a combination of the ion features (ionic size, electronegativity, coordination sphere) operating at the level of the catalytic region and of the ion-driven modifications in overall enzyme structure and flexibility contribute to the mechanism of gyrase activity. An effectual role for DNA recruiting the second catalytic metal ion is envisaged.

The topological changes occurring in bacterial DNA during transcription and replication are managed in part by DNA gyrase (*1*). This enzyme belongs to the type II family of DNA topoisomerases, proteins that change the linking number of circular DNA, performing sequential cleavage and religation steps on both strands of the polynucleotide double helix (*2*). Similarly to other enzymes of this class, gyrase can catalyze several reactions on DNA (i.e., relaxation, decatenation) with different efficiency. However, gyrase is a unique topoisomerase as it is the only member of the family able to introduce negative supercoiling into DNA in a reaction that uses ATP hydrolysis to supply the required energy (*3, 4*).

In its active form gyrase works as a tetramer (A_2B_2) formed by two different proteins, GyrA and GyrB (*5*). Each subunit is involved in specific functions to fully account for the catalytic properties of the reconstituted enzyme. In particular, GyrA, a ~97 kDa protein (875 aa) in *Escherichia coli*, is responsible for DNA binding and wrapping (*6*). Additionally, it contains the catalytic tyrosine (Tyr 122) participating in the covalent reactions with DNA (*5*). GyrB is an ~90 kDa (804 aa) protein and contains the ATP-binding and hydrolysis sites, whereas its C-terminal domain is involved in interactions with GyrA and DNA (*7, 8*). This subunit is characterized by the presence of the TOPRIM fold, a conserved region found also in primases and type IA topoisomerases (*9, 10*). This fold contains a number of acidic residues (Asp and Glu) that are likely involved in the binding of metal ions required in the DNA cleavage reaction (*11*).

The catalytic properties of gyrase are strongly affected by the composition of the reaction buffer (*4, 5*). In particular the enzyme requires Mg^{2+} as a cofactor. To perform some of the reactions catalyzed by the enzyme, Mg^{2+}can be substituted by other divalent metal ions like Ca^{2+} or Mn^{2+}. However, both catalytic efficiency and step progression are modulated by the concentration and the nature of the metal ion (*8, 11, 12*). This can be correlated to the coordination properties of the multiple metal ion binding sites deriving from the protein sequence and folding. Indeed, previous studies revealed that at least two metal ions are required to properly perform the cleavage-resealing cycle (*11*). In this connection, circular dichroism spectroscopy (CD) proved to be a suitable technique to investigate the role of experimental conditions (ions, temperature, drugs) on GyrA and GyrB structure and stability (*13, 14*). For both proteins, we observed specific effects triggered by the presence of divalent

[†] The present work was supported by European Community Grant No. 503466; work in A.M.'s laboratory was also supported by BBSRC (U.K.) and in C.S.'s laboratory by Padova University (Grant No. CPDA078422/07).

* Author to whom correspondence should be addressed. Dept. of Pharmaceutical Sciences, v. Marzolo 5, 35101 Padova, Italy. E-mail: manlio.palumbo@unipd.it.

[‡] University of Padova.

[§] John Innes Centre.

10.1021/bi800480j CCC: $40.75 © 2008 American Chemical Society
Published on Web 07/22/2008

or monovalent metal ions. Based upon these observations, we now investigated the role of the physiologically relevant divalent metal ions Mg^{2+}, Ca^{2+}, Mn^{2+} and Zn^{2+} on the structure and stability of the reconstituted enzyme (A_2B_2). Furthermore, we investigated protein−metal ion complex equilibria in the presence of DNA, given its role as an enzyme substrate and its proposed participation in metal ion coordination during the hydrolytic process (*11*). Indeed, we will show that one of the catalytically relevant metal ions binds to the enzyme independently of DNA, while the second produces the active coordination network only in the presence of the nucleic acid substrate.

MATERIALS AND METHODS

Proteins. All proteins were produced and purified according to previously reported protocols (*11, 13*). Protein purity was assessed by SDS−PAGE; protein concentrations were measured by UV absorbance and by the Bradford protocol (BioRad). The reconstituted enzyme was prepared combining stoichiometric amounts of GyrA and GyrB in the required reaction buffer, and its activity was checked by DNA supercoiling activity.

Metal Ion Solutions. Stock solutions of $Mg(ClO_4)_2$, $Mn(ClO_4)_2$ and $Zn(NO_2)_2$ were prepared freshly in milliQ water.

DNA. Relaxed plasmid pBR322 was prepared by incubating supercoiled pBR322 (Fermentas) with topoisomerase I (Invitrogen) in 50 mM Tris·HCl, pH 7.5, 50 mM KCl, 10 mM $MgCl_2$, 0.5 mM DTT, 100 μM EDTA, 30 μg/mL BSA. A double-stranded DNA fragment of 161 bp was produced by PCR, using pBR322 (2.5 ng) as a DNA template and appropriate primers (0.5 μM) designed to amplify the 906−1065 plasmid sequence. The reaction was carried out in a Perkin-Elmer thermocycler performing 25 cycles of 30 s at 94 °C, 30 s at 65 °C and 30 s at 72 °C. The reaction products were purified with a Qiagen Kit in order to remove primers and nucleotides. The quality of reaction products was evaluated on a 2% agarose gel in TBE 0.5X (45 mM Tris base, 45 mM boric acid, 1 mM Na_2EDTA) and stained with ethidium bromide. The concentration of DNA solution was determined spectrophotometrically.

DNA Supercoiling Assays. Relaxed plasmid pBR322 (0.125 μg) was incubated with DNA gyrase (25 nM) in a total volume of 20 μL in 35 mM Tris·HCl (pH 7.5), 24 mM KCl, 1.8 mM spermidine, 2 mM DTT, 0.1 mg/mL BSA, 1 mM ATP and 6.5% (w/v) glycerol for 30 min at 37 °C in the presence and absence of increasing divalent metal ions concentrations. When required, separate GyrA and GyrB subunits or the enzyme in its reconstituted form were incubated for 2 h at 37 °C with the metal ions before addition of relaxed DNA. Reaction products were resolved on 1% agarose gels in TBE 0.5X and the bands were visualized by ethidium bromide staining and photographed. The relative amounts of different DNA topoisomers were quantified using a BioRad Gel Doc 1000 apparatus interfaced to a PC workstation. The concentration of reconstituted enzyme was increased to 150 and 250 nM when the enzyme was reconstituted with GyrB D500C and GyrB D498A, respectively (*11*). Supercoiling assays were repeated at least in triplicate for each condition described in the text.

Circular Dichroism Measurements. Circular dichroism spectra were recorded using 1−10 mm path length cells on a Jasco J 810 spectropolarimeter in 10 mM Tris·HCl (pH 7.5), 20 mM KCl; when required, divalent metal ions were included in the buffer. For each measurement 3 scans were run and recorded with 1 nm step resolution. Each measurement was repeated at least in triplicate in independent experiments. At the end of each measurement, protein integrity was checked by SDS−PAGE. Observed ellipticities were converted to mean residue ellipticity $[\theta] = \text{deg} \times \text{cm}^2 \times \text{dmol}^{-1}$.

For thermal denaturation experiments, protein solutions (~0.2 μM) were equilibrated at 25 °C, and then the signal at 220 nm was recorded while increasing the temperature at 0.8 °C/min and stirring the protein solution to allow equilibration. Experiments were performed in 10 mM Tris·HCl (pH 7.5), 20 mM KCl in the presence or absence of different concentration of metal ions. T_m was determined locating the maxima/minima of the first derivative of the curve describing the melting profile (CD vs *T*). To estimate the amount of protein secondary structure, CD spectra ranging from 200 to 240 nm were analyzed using the K2D neural network (*15*); when required 1 equiv of DNA was added to the protein solutions before metal ion additions.

RESULTS

Metal Ions Remarkably Affect Reconstituted DNA Gyrase Structure and Stability. GyrA and GyrB had been previously characterized in terms of protein folding and melting profile in solution (*13, 14, 16*). However, extensive subunit interactions occurring in the reconstituted enzyme might affect the properties of the individual components. Thus, we examined the reconstituted enzyme in the presence and absence of divalent metal ions. CD measurements in 10 mM Tris·HCl (pH 7.5), 20 mM KCl, showed that at 25 °C the spectrum of the reconstituted enzyme corresponds to the sum of the contributions from the separate domains (Figure 1A) and accounts for 31% α-helix, 11% β-sheet and 58% random coil. The same is true in the presence of 4 mM Ca^{2+} or Mg^{2+}. Indeed, these components are apparently not affecting either GyrA (not shown) or GyrB (*14*) folding equilibria at room temperature.

By contrast, addition of the catalytically effective Mn^{2+} to the A_2B_2 complex induces large structural rearrangements as shown by an extensive change in the protein optical activity (Figure 1B). This is reminiscent of the behavior of GyrB (*14*) since Mn^{2+} ions do not induce significant conformational changes in GyrA at room temperature (data not shown). In the presence of Zn^{2+}, extensive protein precipitation occurs thus preventing any spectroscopic characterization of the complex(es).

The melting profile of the reconstituted enzyme is presented in Figure 2A. Working at 220 nm in 10 mM Tris·HCl (pH 7.5), 20 mM KCl, 4 distinct thermal transitions with T_m at 41.4 °C, 49.5 °C, 54.5 and 61.5 °C were recorded, in good agreement with data obtained using the differential scanning calorimetry technique (*16*). When monitoring the thermal stability of the reconstituted protein in the presence of divalent metal ions, we generally observed a shift of the protein structural transitions to lower temperature (Figure 2A). The experimental ranking order of efficiency is $Mn^{2+} > Mg^{2+} > Ca^{2+}$. Interestingly, this order matches the one observed with the separate subunits although enzyme recon-

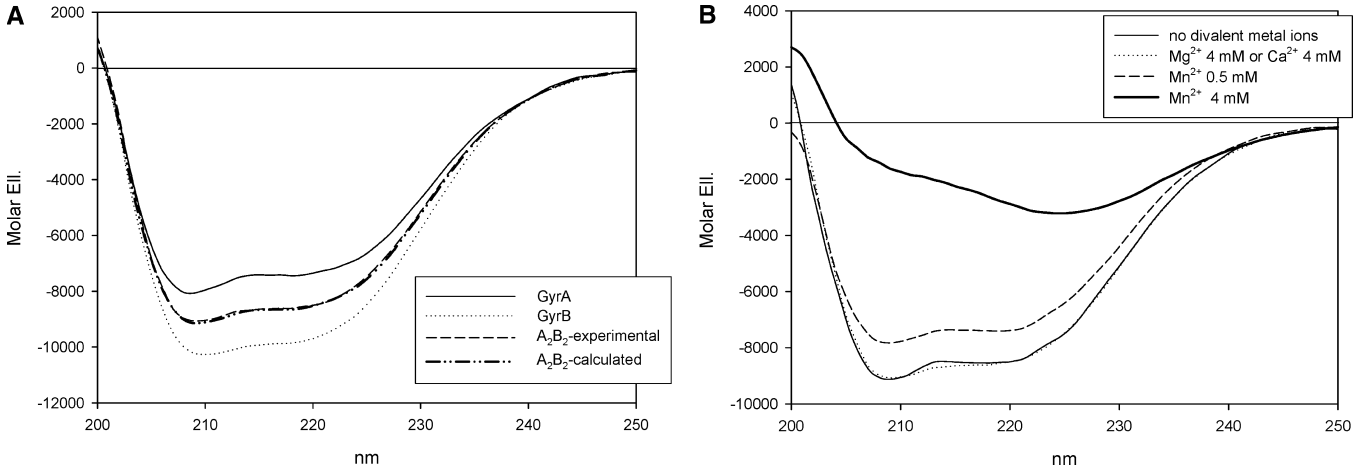

FIGURE 1: Conformational properties of DNA gyrase. Panel A: Circular dichroism (CD) spectra at 25 °C of GyrA, GyrB and A_2B_2 (0.2 μM each) recorded in 10 mM Tris·HCl (pH 7.5), 20 mM KCl. Data resulting from the linear composition of the spectra of the single domains (GyrA + GyrB) is also included. Panel B: CD spectra of A_2B_2 (0.2 μM) in 10 mM Tris·HCl (pH 7.5), 20 mM KCl, in the presence of different concentrations of divalent metal ions after extensive equilibration at 25 °C.

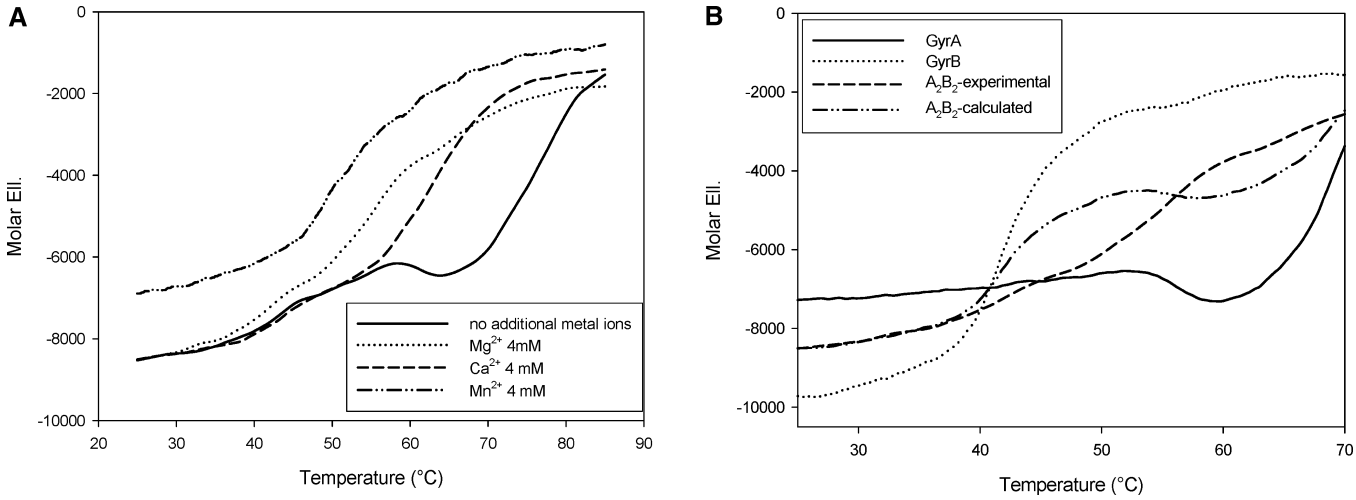

FIGURE 2: Thermal stability of DNA gyrase. Panel A: A_2B_2 (0.2 μM) thermal melting profile recorded from the dichroic signal at 220 nm in 10 mM Tris·HCl (pH 7.5), 20 mM KCl, in the presence/absence of divalent metal ions (4 mM). Panel B: CD melting profiles at 220 nm of 0.2 μM GyrA (solid line), 0.2 μM GyrB (dotted line) and 0.05 μM A_2B_2 (dashed line) recorded in 10 mM Tris·HCl (pH 7.5), 20 mM KCl, 4 mM Mg^{2+}. The data resulting from the linear composition of the spectra of the single domains (GyrA + GyrB, dashed-dotted line) is also included.

stitution makes the differences between Mg^{2+} and Ca^{2+} less remarkable (*14*).

Increasing the temperature above 40 °C leads to a CD signal stronger than the one derived from the sum of GyrA and GyrB contributions both in the presence and in the absence of divalent metal ions confirming a mutual interaction between the GyrA and GyrB subunits. This appears clearly by comparing the experimentally recorded A_2B_2 melting profile with the linear combination of the profiles relative to the separate domains in the presence/absence of divalent metal ions (Figure 2B). At temperatures higher than 55 °C the melting profiles tend to merge. The melting experiments do not show evidence of any new transition attributable to the dissociation of the tetrameric complex. However, the GyrB melting transition, occurring at ~40 °C in the isolated subunit, is remarkably shifted to higher temperatures in the reconstituted tetramer.

Mn^{2+} Forms Two Types of Complex with DNA Gyrase. Among the test metal ions, only Mn^{2+} is able to induce appreciable modifications to the protein structure. An accurate monitoring of the gyrase−Mn^{2+} binding process shows that the protein can assume two distinct conformational states as a function of metal ion concentration (Figure 1B): at low Mn^{2+} (<2 mM) a complex producing modest change in ellipticity is observed. By increasing the metal ion concentration, a second process occurs, which affects the higher energy CD band (210 nm) to a larger extent than the 220 nm band, giving rise to a new species with a maximum located at 225 nm. A conformational analysis of this complex is consistent with a large reduction in α-helix content (from 31 to 5%). The protein conversion into this structure is a slow process, and the time required to reach the final state is inversely related to temperature and metal ion concentration. The above dramatic changes are not connected with protein aggregation, precipitation or photolytic cleavage events as indicated by light-scattering and SDS−PAGE experiments (data not shown).

The analysis of the protein conformational change as a function of the metal ion/protein ratios allowed us to evaluate the complex stoichiometry. The data relative to the first process are presented in Figure 3. They are consistent with a 1:1 stoichiometry suggesting that the first Mn^{2+} ion binds

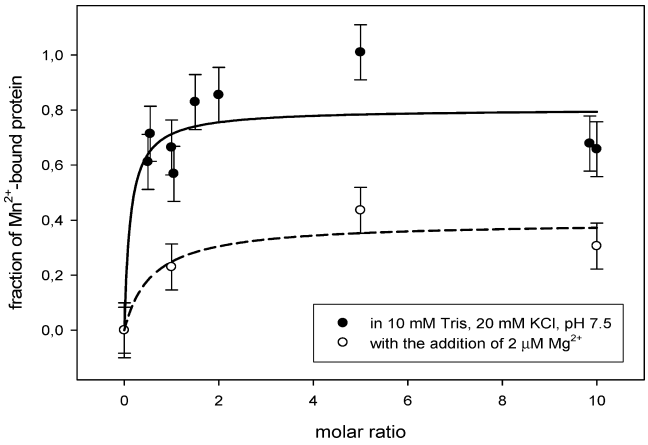

FIGURE 3: The first process of Mn^{2+} binding to DNA gyrase corresponds to a 1:1 stoichiometry. Percentage of Mn^{2+}-bound GyrB as a function of protein:metal ion molar ratio. Fractions were calculated monitoring changes in the CD of GyrB at 220 nm after incubation in 10 mM Tris·HCl (pH 7.5), 20 mM KCl, at 25 °C (full symbols) or in the same buffer in the presence of 2 μM Mg^{2+} (empty symbols).

to the enzyme without causing major structural modification. It is worth noting that Mg^{2+} can compete with Mn^{2+} for this binding site. Indeed, when we analyzed the Mn^{2+}-mediated structural transition of the protein in the presence of Mg^{2+} at a stoichiometric ratio, we observed a drop in the amount of protein undergoing the first structural rearrangement (not shown).

The second binding process exhibits a lower formation constant as indicated by the excess of metal ion required to reach saturation. Under these conditions the stoichiometry of the second process is hard to determine.

DNA Substrate Affects the DNA Gyrase−Mn^{2+} Equilibria. To assess the role of nucleic acid on gyrase we used a 191 bp fragment containing a hot spot for DNA cleavage by the enzyme corresponding to position 990 in pBR322 (*17*). Generally, addition of DNA did not produce appreciable modifications in the CD spectra of GyrA, GyrB and reconstituted gyrase in the presence or absence of Mg^{2+} ions. Again a notable exception occurs when Mn^{2+} is included. The presence of nucleic acid is not apparently influencing the folding of the reconstituted enzyme at room temperature. However, upon raising the temperature to the physiologically significant 37 °C, the minor Mn^{2+}-driven conformational changes in A_2B_2 corresponding to the 1:1 stoichiometry still occur, whereas the dramatic transition to the second type of complex is no longer observed (Figure 4). A detailed analysis of the melting profiles obtained from ternary protein−metal ion−DNA combinations cannot be performed due to the presence of several overlapping transitions.

Divalent Metal Ions Affect Protein Activity. Since all tested divalent metal ions reduce protein stability to an extent related to their nature and concentration, we examined the catalytic activity of reconstituted DNA gyrase in the presence of various amounts of Ca^{2+}, Mg^{2+}, Mn^{2+} and Zn^{2+}, performing supercoiling assays. As reported above, Zn^{2+}-mediated protein precipitation prevents detection of any catalytic activity. With the other test metals, we found a bell-shaped dependence of enzyme supercoiling activity as a function of metal ions concentrations, in agreement with literature data (Figure 5) (*8, 11*). Maximal enzyme activity is monitored

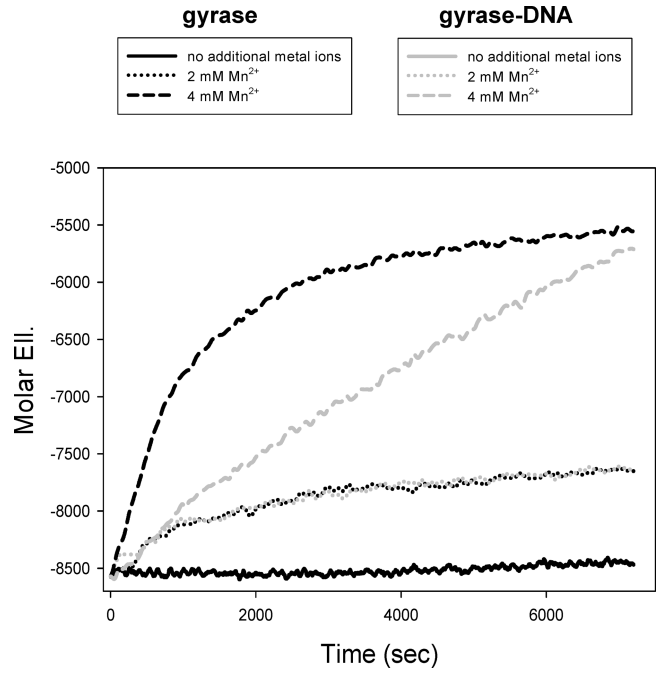

FIGURE 4: DNA reduces Mn^{2+}-driven gyrase structural modifications. CD intensity recorded at 220 nm for gyrase (0.05 μM) is reported as a function of incubation time in the presence of variable amounts of Mn^{2+}. Data were collected in the absence (black lines) or the presence (gray lines) of 0.05 μM dsDNA in 10 mM Tris·HCl (pH 7.5), 20 mM KCl, at 37 °C.

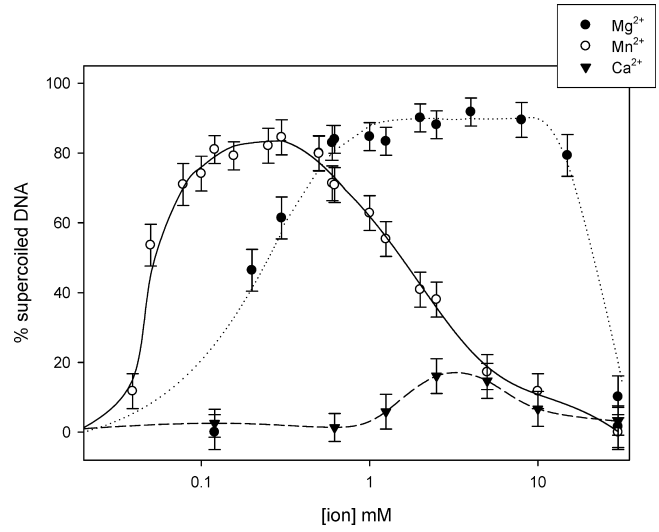

FIGURE 5: Divalent metal ions modulate the DNA supercoiling activity of DNA gyrase in terms of maximal response and activity concentration window. Percentage of supercoiled DNA obtained incubating relaxed pBR322 (0.125 μg) for 30 min at 37 °C with DNA gyrase (25 nM) in the presence of increasing concentrations of divalent metal ions.

at comparable Ca^{2+} or Mg^{2+} concentrations, whereas it is shifted to lower concentrations in the presence of Mn^{2+}. Interestingly, the latter metal ion shows an extremely narrow activity window, which produces almost complete loss of enzymatic catalysis at 4 mM. Additionally, at concentrations that allow maximal enzyme activity, the amount of supercoiled product, comparable for Mg^{2+} and Mn^{2+}, is substantially reduced in the presence of Ca^{2+} (Figure 5).

Mn^{2+}-Driven Gyrase Conformational Rearrangements Impair Enzyme Activity. Chiroptical studies showed that protein structural changes induced by the presence of Mn^{2+}

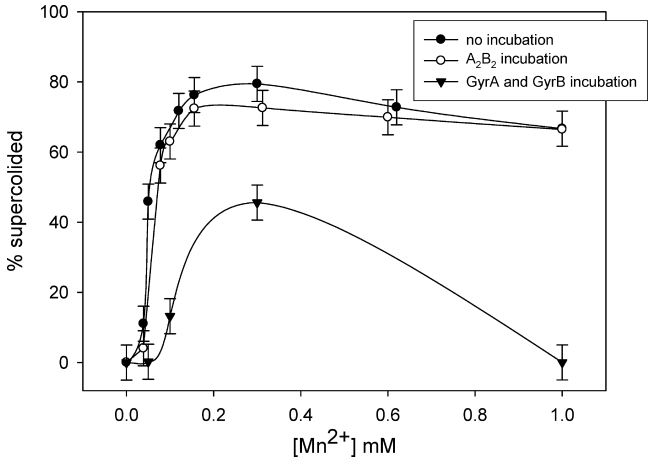

FIGURE 6: Mn^{2+}-mediated structural rearrangements of GyrB impair DNA gyrase activity. Effect of increasing concentrations of divalent metal ions on the supercoiling activity of DNA gyrase (25 nM). Reactions were performed incubating for 30 min at 37 °C relaxed pBR322 (0.125 μg) immediately after metal ion additions to the reconstituted enzyme (full circles) or after 2 h incubation at 37 °C (empty circles), and after addition of the metal ion to the separate subunits following 2 h incubation at 37 °C (triangles).

occur slowly and that this rate is further substantially reduced in the presence of DNA. Hence, we tested gyrase activity after incubation with this metal ion for the time required to allow protein folding rearrangements to fully occur. No significant changes in the catalytic properties were observed when the reconstituted protein was incubated with the required metal ion concentration up to two hours before addition of the relaxed DNA substrate. Notably, the divalent metal ion concentrations at which gyrase showed significant supercoiling activity are in the range where only the first complex is formed even at 37 °C (<2 mM). Subsequently, we incubated the two enzyme subunits with Mn^{2+}separately at 37 °C before enzyme reconstitution and DNA addition, thus using conditions at which CD data showed the presence of the less ordered structure. Indeed, using this experimental protocol we observed an extensive suppression in gyrase enzymatic activity (Figure 6). On the contrary, by replacing Mn^{2+} with Mg^{2+}, no variation in catalytic activity was observed upon prior incubation of the two subunits with the metal ion. Recalling that manganese ions do not appreciably change the GyrA active conformation, this suggests that the Mn^{2+}-driven (GyrB) structural rearrangement corresponding to the second type of complex impairs enzyme activity.

As we observed competition between Mg^{2+} and Mn^{2+} for the first binding event, we performed protein activity assays (Figure 7), using metal ion concentrations at which maximal supercoiling activity was observed (0.5 and 4 mM for Mn^{2+} and Mg^{2+} respectively). Interestingly, when the protein was previously equilibrated with an excess of Mg^{2+} (4 mM), the low Mn^{2+} concentration (0.5 mM) is sufficient to induce the protein structural modification associated with the second metal ion binding event (Figure 7A). As a consequence, the simultaneous presence of the metal ions at the above concentrations largely impairs protein efficiency, recalling the behavior of the enzyme at high concentrations of Mn^{2+} in the absence of Mg^{2+}.

Mn^{2+} Interference with the TOPRIM Region Modulates DNA Gyrase Supercoiling Activity. To further define the role of metal ion complexation, chiroptical and activity assays were performed using two site-directed TOPRIM mutants characterized by different affinities for Mn^{2+}: in D500C a sulfur atom is introduced into the divalent metal ion coordination site/s in an effort to shift binding preference toward soft Lewis acids like manganese ions. By contrast, in D498A, a potential metal ion coordination ligand (a carboxyl group) is removed. Indeed, D500C with the sulfur atom participating in the ion coordination sphere showed a higher affinity for manganese than the wt protein and D498A with the neutral amino acid exhibited lower affinity (*11, 14*). Although with a reduced efficiency, both mutants yielded active enzymes when reconstituted with GyrA, and the expected modulation in activity due to the nature of divalent metal ion was observed. Here, we compared the structural transitions these proteins undergo upon incubation with Mn^{2+}. As reported in Figure 8, the order of affinity for this metal ion parallels the extent of changes in chiroptical properties observed with the wt and mutant GyrB subunits. This allowed us to test forms of the enzyme exhibiting different degree of GyrB conformational rearrangement. Interestingly, we found the maximal drop in supercoiling activity after incubation of D500C with Mn^{2+}, whereas activity was largely retained by the enzyme reconstituted with the D498A−Mn^{2+} complex (Figure 9).

DISCUSSION

The catalytic steps through which DNA gyrase produces its biological action have been thoroughly investigated in previous work (*18, 19*). Although detailed three-dimensional information is currently available for portions of GyrA and GyrB, this is not sufficient to propose a structure for the tetrameric enzyme (*20–24*). In fact, it is very hard to model the extensive protein−protein interactions at the interface between subunits as well as the large conformational changes occurring during the catalytic cycle. Additionally, the physiological environment affects the biological properties of gyrase, a key role being played by metal ion cofactors that are crucial to bestow and modulate catalytic activity.

The spectroscopic studies presented here suggest that the individual structures of GyrA and GyrB are essentially preserved in the reconstituted enzyme. However, the presence of significant interactions among the subunits clearly emerged by monitoring the enzyme melting profile; A_2B_2 complex formation produced an increase in protein stability. In particular, GyrB appeared to be profoundly stabilized by this process. Taking into account that GyrA *per se* is stable up to 55 °C (*13, 25*), we propose that the formation of the tetrameric complex allows GyrB to be anchored onto the thermally more stable GyrA thus reducing its intrinsic flexibility. Indeed, when the reconstituted enzyme was incubated at a temperature at which GyrA melts, the CD spectrum corresponded to the sum of the spectra recorded with the isolated subunits, further suggesting that upon GyrA denaturation the A_2B_2 complex falls apart producing the isolated components (*25*).

Metal ion binding to the reconstituted enzyme does not remarkably alter protein conformation at physiological conditions, with the notable exception of Mn^{2+}. Similar effects were shown by GyrB, whereas GyrA did not undergo structural rearrangements with the same ion (*11, 14*). It is worth mentioning that the reconstituted enzyme requires

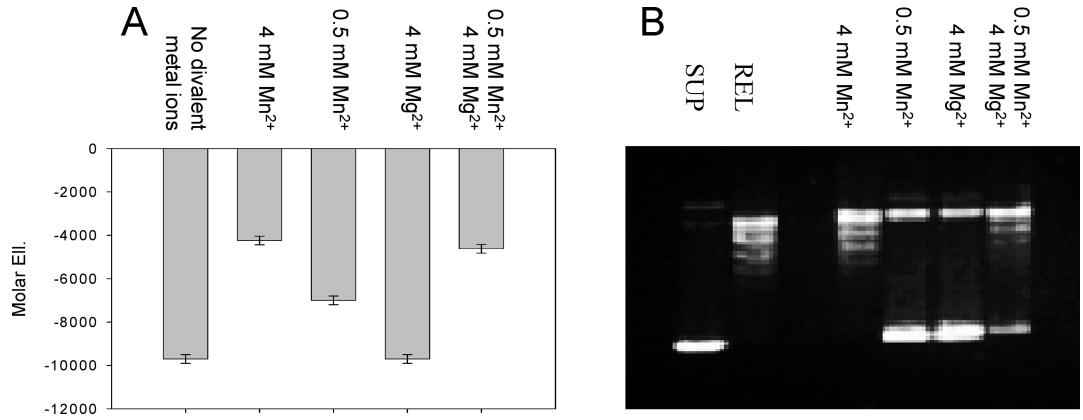

FIGURE 7: Mg^{2+} affects the Mn^{2+}-driven protein conformational and activity changes. Panel A: Molecular ellipticity for GyrB recorded at 220 nm in 10 mM Tris·HCl (pH 7.5), 20 mM KCl at 25 °C, in the presence/absence of Mg^{2+} and/or Mn^{2+} at the reported concentrations. Panel B: DNA gyrase supercoiling activity assay in the presence/absence of the same amount of metal ions as in panel A. Reactions were performed at 37 °C incubating relaxed pBR322 (0.125 μg) with 25 nM DNA gyrase for 30 min after metal ion additions. Lane marked SUP represents supercoiled plasmid; lane marked REL represents relaxed plasmid.

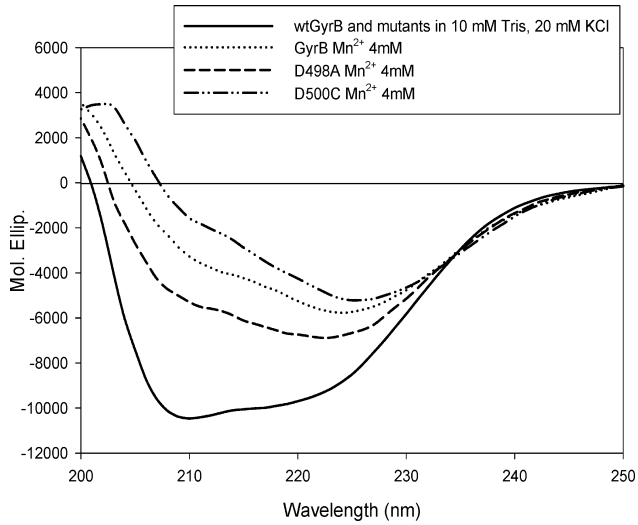

FIGURE 8: TOPRIM mutants are differentially affected by Mn^{2+}. Effect of increasing concentrations of Mn^{2+} on the CD spectra of wtGyrB, D498A and D500C (0.2 μM each) recorded in 10 mM Tris·HCl (pH 7.5), 20 mM KCl, 4 mM Mn^{2+} at 25 °C.

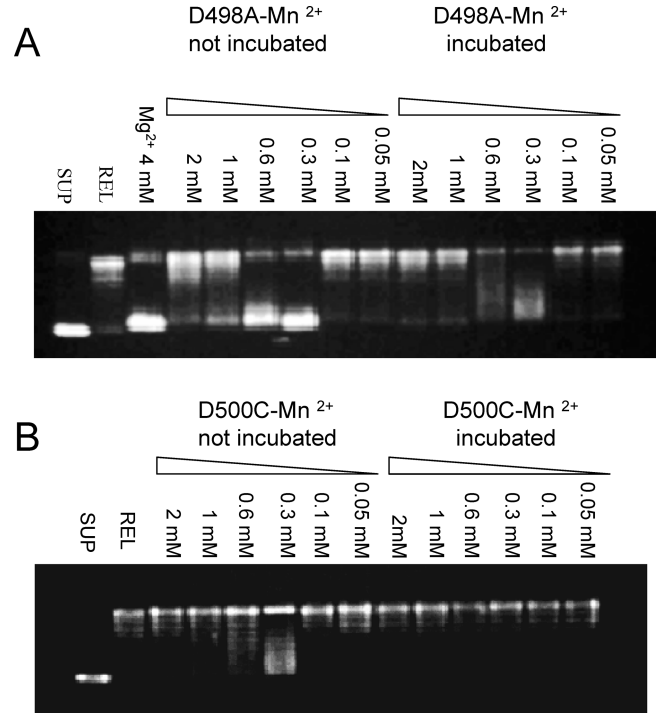

FIGURE 9: Effect of increasing concentrations of Mn^{2+} on the supercoiling activity of DNA gyrase reconstituted with GyrB D498A (250 nM, panel A) or GyrB D500C (150 nM, panel B). Reactions were performed at 37 °C incubating relaxed pBR322 (0.125 μg) 30 min after metal ion additions to the separate subunits (left side, no incubation) or after 2 h of incubation at 37 °C (right side, incubation). Lanes marked SUP represent supercoiled plasmid; lanes marked REL represent relaxed plasmid.

higher metal ion concentrations to produce structural changes comparable to those in GyrB, which confirms a scaffold role of GyrA in regulating the enzyme conformation.

Chiroptical studies show two distinct changes as a function of Mn^{2+} concentration, which indicates the presence of at least two discrete metal ion binding sites, each affecting protein folding to a different extent. In previous studies, we proved that Mn^{2+}-mediated structural modifications are due to metal ion binding at site(s) other than the ATPase domain and proposed a specific interaction of two metal ions with the TOPRIM domain in GyrB47, thereby assisting the DNA cleavage reaction (*11, 14*). Two-metal ion-mediated mechanisms are reported for most enzymes performing DNA phosphoryl-transfer reactions (*26*). Our previous findings are fully consistent with those observed using A_2B_2 and lead us to conclude that the two distinct conformationally relevant binding events occur in the TOPRIM region. The first structural transition can be safely associated with a 1:1 stoichiometry, while the subsequent, more dramatic, conformational change is ascribable to the second coordination event.

The chemical similarity of Mg^{2+} and Mn^{2+} (*27*) suggests a comparable geometry in the 1:1 complex with gyrase. In fact, competition between Mg^{2+} and Mn^{2+} for this site has been clearly evidenced in the chiroptical studies. On the contrary, further metal ion binding shows opposite effects, Mg^{2+} still stabilizing the active structure and Mn^{2+} distorting it to a substantial extent and leading to an inactive enzyme. In the absence of sufficient O-containing ligands (the two metal ions should be very close in space (*11*)) Mn^{2+} can rely on its ability to coordinate nitrogen-containing ligand(s) eventually producing a dramatic change in protein conformation, while Mg^{2+} fails to do so. Interestingly, in the presence

Scheme 1: Proposed Model for Two-Metal Ion-Mediated DNA Gyrase Action[a]

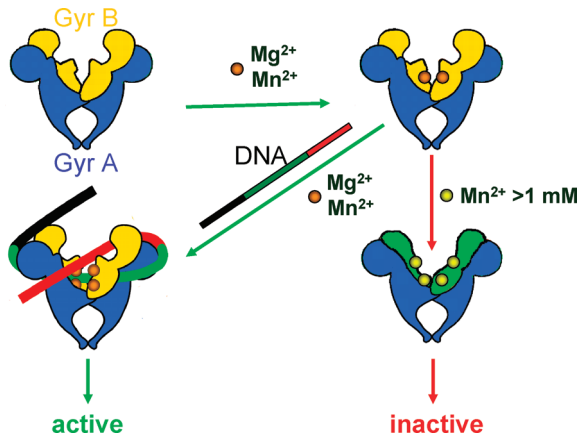

[a] The first ion binding site is already present in each B subunit of the reconstituted enzyme, while the second, needed for catalysis, is generated in the presence of the nucleic acid. Forcing the metal ion to occupy this latter site in the absence of the target substrate leads to inactive enzyme conformation. Colors in the DNA molecule are as follows: green, gate segment; red, transfer segment.

of Mg^{2+}, Mn^{2+} tends to occupy this second site only, which also suggests that Mg^{2+} probably does not normally bind to it or binds with a substantially reduced affinity.

In the presence of DNA, the nucleic acid bound to the protein is able to provide additional oxygen-containing (phosphate) coordination site(s), activating the second Mg^{2+}-binding event required for catalysis. Under these circumstances, the second Mn^{2+} can form a stable complex in a way similar to Mg^{2+} with no need for protein distortion, as confirmed by the high catalytic efficiency when adding the metal ion with the substrate DNA and, conversely, the substantial loss in activity when incubating the subunits with Mn^{2+} prior to reconstitution. Maintenance of the gyrase effective conformation explains preservation of catalytic activity. Moreover, the similarity in complexation pattern accounts for the similar maximal response shown by Mn^{2+} and Mg^{2+}. However, when the concentration of Mn^{2+} exceeds 0.5 mM, competition between the active and inactive protein conformation (second type of complex) becomes more likely and a pronounced activity drop occurs. Saturation of the first binding site with Mg^{2+} allows Mn^{2+} to be directed to the second binding site only, thus producing a conformational shift toward the inactive form and impairing catalytic activity even at low metal ion concentration.

A schematic representation of the conformational/catalytic events occurring during metal ion binding to DNA gyrase in the presence of the ion cofactors and DNA is outlined in Scheme 1.

Notwithstanding its close similarity with Mg^{2+}, Ca^{2+} performs poorly as a gyrase cofactor. According to crystallographic data on polymerases and nucleases reported to date, the closest approach between two Ca^{2+} ions is observed at 3.8 Å, whereas it is below 3.0 Å for Mn^{2+} and Mg^{2+} (*27*). This longer distance could impair the concerted two-ion mechanism. In addition, binding of Ca^{2+} to gyrase should distort the optimal steric and electronic requirements of the catalytic transition state, hence raising its energy. In fact, recent *ab initio* studies on the mechanism by which magnesium, but not calcium ions, coadjuvate the *Bam*HI enzyme in cleaving the phosphodiester bond in DNA showed that a concerted two-metal mode of action leads to a transition state remarkably more stable in the presence of magnesium than in the presence of calcium (*28*). Furthermore, it is worth noting that, besides sustaining DNA supercoiling by gyrase, Ca^{2+} also stabilizes the cleavage complex in a manner similar to quinolone drugs (*29*). This suggests that Ca^{2+} can support DNA cleavage by gyrase but is less effective than Mg^{2+} in supporting religation. This is consistent with Ca^{2+} ability to allow fast water exchange for other binding groups, which is not true for Mg^{2+} (*30*). Replacement of the nucleoside hydroxyl involved in phosphodiester bond resealing with a water molecule in the Ca^{2+} coordination sphere would render transesterification no longer feasible and produce effects similar to a topoisomerase poison.

Studies on two GyrB mutants are in line with this proposal and underline a differential role played by residues at position 498 and 500. Our present results suggest that residue D498 participates in the coordination sphere of the second type Mn^{2+} complex, since the D−A substitution leads to a substantial drop in affinity (and activity) for this ion. On the other hand, mutations at residue D500 affect the binding of all test divalent ions, although to different extents, which suggests its involvement in the first complexation event.

The crystal structure of the DNA-binding and cleavage core of *Saccharomyces cerevisiae* type IIA topoisomerase bound to prospective gate-segment DNA has been recently reported and the structural organization of the catalytic site dissected at atomic resolution (*31*). In total agreement with our findings, a magnesium ion is modeled at the level of the TOPRIM E450, D527 and D529 residues corresponding to the *E. coli* GyrB residues E424, D498 and D500, which were proposed to be involved in metal ion binding and the mutation of which substantially affected DNA gyrase catalytic properties. Although a second metal ion could be located in the catalytic site of the yeast topoisomerase, this is probably lacking in the crystal structure because of the absence of a scissile phosphate in the cleavage position of the oligonucleotide substrate (*29*). Indeed, as we showed here, the second metal ion needs the presence of the DNA phosphate to be appropriately coordinated in the catalytic pocket.

In conclusion, the effects of divalent metal ions on DNA gyrase activity can be rationalized as a combination of the ion features (ionic size, electronegativity, coordination preferences) operating at the level of the TOPRIM region and of the ion-driven modifications in overall enzyme structure and flexibility, both of which largely impact the activation free energy barrier and the recrossing of it (*32*). At the same time, data herein reported suggest an active role played by DNA within the gyrase catalytic complex. Indeed, the nucleic acid, far from acting as a passive substrate, represents a crucial component to properly recruit the cofactors (metal ions) needed to perform gyrase catalytic cycle.

ACKNOWLEDGMENT

We thank Christian Noble for gifts of proteins.

REFERENCES

1. Levine, C., Hiasa, H., and Marians, K. J. (1998) DNA gyrase and topoisomerase IV: biochemical activities, physiological roles during chromosome replication and drug sensitivities. *Biochim. Biophys. Acta 1400*, 29–43.
2. Champoux, J. J. (2001) DNA Topoisomerases: Structure, function and mechanism. *Annu. Rev. Biochem. 70*, 369–413.
3. Cozzarelli, N. R. (1980) DNA gyrase and the supercoiling of DNA. *Science 207*, 953–960.
4. Gellert, M., Mizuuchi, K., O'Dea, M. H., and Nash, H. A. (1976) DNA gyrase: an enzyme that introduces superhelical turns into DNA. *Proc. Natl. Acad. Sci. U.S.A. 73*, 3872–3876.
5. Reece, R. J., and Maxwell, A. (1991) DNA gyrase: structure and function. *CRC Crit. Rev. Biochem. Mol. Biol. 26*, 335–375.
6. Sugino, A., Peebles, L. C., Kreuzer, K. N., and Cozzarelli, N. R. (1978) Mechanism of action of nalidixic acid: Purification of *Escherichia coli nalA* gene product and its relationship to DNA gyrase and a novel nicking-closing enzyme. *Proc. Natl. Acad. Sci. U.S.A. 74*, 4767–4771.
7. Mizuuchi, K., O'Dea, M. H., and Gellert, M. (1978) DNA gyrase: subunit structure and ATPase activity of the purified enzyme. *Proc. Natl. Acad. Sci. U.S.A. 75*, 5960–5963.
8. Sugino, A., and Cozzarelli, N. R. (1980) The intrinsic ATPase of DNA gyrase. *J. Biol. Chem. 255*, 6299–6306.
9. Aravind, L., Leipe, D. D., and Koonin, E. V. (1998) Toprim - a conserved catalytic domain in type IA and II topoisomerases, DnaG-type primases, OLD family nucleases and RecR proteins. *Nucleic Acids Res. 26*, 4205–4213.
10. Podobnik, M., McInerney, P., O'Donnell, M., and Kuriyan, J. (2000) A TOPRIM domain in the crystal structure of the catalytic core of Escherichia coli primase confirms a structural link to DNA topoisomerases. *J. Mol. Biol. 300*, 353–362.
11. Noble, C. G., and Maxwell, A. (2002) The role of GyrB in the DNA cleavage-religation reaction of DNA gyrase: a proposed two metal-ion mechanism. *J. Mol. Biol. 318*, 361–371.
12. Cullis, P. M., Maxwell, A., and Weiner, D. P. (1997) Exploiting nucleotide thiophosphates to probe mechanistic aspects of Escherichia coli DNA gyrase. *Biochemistry 36*, 6059–6068.
13. Sissi, C., Perdonà, E., Domenici, E., Feriani, A., Howells, A. J., Maxwell, A., and Palumbo, M. (2001) Ciprofloxacin affects conformational equilibria of DNA gyrase A in the presence of magnesium ions. *J. Mol. Biol. 311*, 195–203.
14. Sissi, C., Marangon, E., Chemello, A., Noble, C. G., Maxwell, A., and Palumbo, M. (2005) The effects of metal ions on the structure and stability of the DNA gyrase B protein. *J. Mol. Biol. 353*, 1152–1160.
15. Andrade, M. A., Chacón, P., Merelo, J. J., and Morán, F. (1993) Evaluation of secondary structure of proteins from UV circular dichroism using an unsupervised learning neural network. *Protein Eng. 6*, 383–390.
16. Blandamer, M. J., Briggs, B., Cullis, P. M., Jackson, A. P., Maxwell, A., and Reece, R. J. (1994) Domain structure of Escherichia coli DNA gyrase as revealed by differential scanning calorimetry. *Biochemistry 33*, 7510–7516.
17. Lockshon, D., and Morris, D. R. (1985) Sites of reaction of Escherichia coli DNA gyrase on pBR322 in vivo as revealed by oxolinic acid-induced plasmid linearization. *J. Mol. Biol. 181*, 63–74.
18. Schoeffler, A. J., and Berger, J. M. (2005) Recent advances in understanding structure-function relationships in the type II topoisomerase mechanism. *Biochem. Soc. Trans. 33*, 1465–1470.
19. Maxwell, A., Costenaro, L., Mitelheiser, S., and Bates, A. D. (2005) Coupling ATP hydrolysis to DNA strand passage in type IIA DNA topoisomerases. *Biochem. Soc. Trans. 33*, 1460–1464.
20. Morais Cabral, J. H., Jackson, A. P., Smith, C. V., Shikotra, N., Maxwell, A., and Liddington, R. C. (1997) Crystal structure of the breakage-reunion domain of DNA gyrase. *Nature 388*, 903–906.
21. Costenaro, L., Grossmann, J. G., Ebel, C., and Maxwell, A. (2005) Small-angle X-ray scattering reveals the solution structure of the full-length DNA gyrase A subunit. *Structure 13*, 287–296.
22. Wigley, D. B., Davies, G. J., Dodson, E. J., Maxwell, A., and Dodson, G. (1991) Crystal structure of an N-terminal fragment of the DNA gyrase B protein. *Nature 351*, 624–629.
23. Lewis, R. J., Singh, O. M., Smith, C. V., Skarzynski, T., Maxwell, A., Wonacott, A. J., and Wigley, D. B. (1996) The nature of inhibition of DNA gyrase by the coumarins and the cyclothialidines revealed by X-ray crystallography. *EMBO J. 15*, 1412–1420.
24. Costenaro, L., Grossmann, J. G., Ebel, C., and Maxwell, A. (2007) Modular structure of the full-length DNA gyrase B subunit revealed by small-angle X-ray scattering. *Structure 15*, 329–339.
25. Maxwell, A., and Gellert, M. (1984) The DNA dependence of the ATPase activity of DNA gyrase. *J. Biol. Chem. 259*, 14472–14480.
26. Yang, W., Lee, J. Y., and Nowotny, M. (2006) Making and breaking nucleic acids: two-Mg^{2+}-ion catalysis and substrate specificity. *Mol. Cell 22*, 5–13.
27. Bock, C. W., Katz, A. K., Markham, G. D., and Glusker, J. P. (1999) Manganese as a replacement for magnesium and zinc: functional comparison of the divalent ions. *J. Am. Chem. Soc. 121*, 7360–7372.
28. Mordasini, T., Curioni, A., and Andreoni, W. (2003) Why do divalent metal ions either promote or inhibit enzymatic reactions. *J. Biol. Chem. 278* 4381–4384.
29. Reece, R. J., and Maxwell, A. (1989) Tryptic fragments of the Escherichia coli DNA gyrase A protein. *J. Biol. Chem. 264*, 19648–19653.
30. Williams, R. T. (1999) Calcium: the developing role of its chemistry in biological evolution, in *Calcium as a cellular regulator* (Carafoli, E., and Klee, C. B., Eds.) pp 3−27, Oxford University Press, New York.
31. Dong, K. C., and Berger, J. M. (2007) Structural basis for gate-DNA recognition and bending by type IIA topoisomerases. *Nature 450*, 1201–1206.
32. Hammes-Schiffer, S. (2002) Impact of enzyme motion on activity. *Biochemistry 41*, 13335–13343.

BI800480J